

Strengthening of axially loaded concrete columns using stainless steel wire mesh (SSWM)-numerical investigations

Varinder Kumar^{*1} and P.V. Patel^{2a}

¹Department of Civil Engineering, Nirma University, Ahmedabad, India

²Department of Civil Engineering, Institute of Technology, Nirma University, Ahmedabad, India

(Received March 7, 2016, Revised September 24, 2016, Accepted October 5, 2016)

Abstract. Stainless steel wire mesh (SSWM) is an alternative material for strengthening of structural elements similar to fiber reinforced polymer (FRP). Finite element (FE) method based Numerical investigation for evaluation of axial strength of SSWM strengthened plain cement concrete (PCC) and reinforced cement concrete (RCC) columns is presented in this paper. PCC columns of 200 mm diameter with height 400 mm, 800 mm and 1200 mm and RCC columns of diameter 200 mm with height of 1200 mm with different number of SSWM wraps are considered for study. The effect of concrete grade, height of column and number of wraps on axial strength is studied using finite element based software ABAQUS. The results of numerical simulation are compared with experimental study and design guidelines specified by ACI 440.2R-08 and CNR-DT 200/2004. As per numerical analysis, an increase in axial capacity of 15.69% to 153.95% and 52.39% to 109.06% is observed for PCC and RCC columns respectively with different number of SSWM wraps.

Keywords: stainless steel wire mesh; axial strength; finite element method; wrap; circular columns

1. Introduction

Most of the concrete structures need to be retrofitted due to change in usage of the structure for enhanced performance during their service life, the old structures being structurally unsafe as per new design codes and decay caused by premature deterioration of structures etc. There are two possible solutions to this problem either replacement or retrofitting. It is more economical to retrofit the structures which require less time, less labour cost and less material cost than to replace it with new ones.

The capacity of existing columns needs to be enhanced when there is an increase in loading due to changes in usage or change in design specifications. Steel and concrete jacketing has been used since long for retrofitting of columns. Fiber Reinforced Polymer (FRP) wrapping is emerging as new method for strengthening of columns. Common types of FRP for wrapping is carbon fiber reinforced polymer (CFRP), glass fiber reinforced polymer (GFRP), and aramid fiber reinforced polymer (AFRP) as shown in Fig. 1(a), (b) and (c). Stainless steel wire mesh (SSWM), as shown

*Corresponding author, Ph.D. Research Scholar, E-mail: vksongc@gmail.com

^aProfessor, E-mail: Paresh.Patel@nirmauni.ac.in

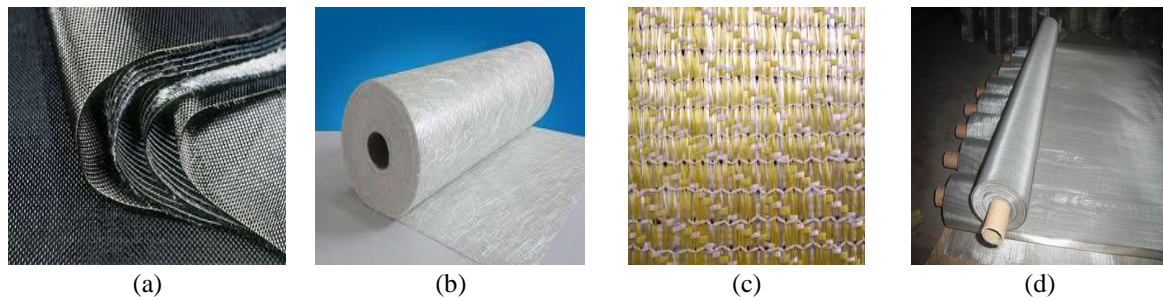


Fig. 1 (a) Carbon fiber reinforced polymer, (b) Glass fibre reinforced polymer (c) Aramid fibre reinforced polymer (d) Stainless steel wire mesh (SSWM)

in Fig. 1(d), with epoxy binder has been introduced as a new class of composites for strengthening applications. The steel wires that make up SSWM have some inherent ductility. SSWM has advantage of being relatively lightweight in comparison to steel plates, making it relatively easy to install. It is also economical as compared to GFRP or CFRP.

SSWM is an alternative to GFRP/CFRP and is made up of high strength steel wires as shown in Fig. 1(d). SSWM is used as an external reinforcement which can be glued to the concrete using epoxy. In contradiction to glass and carbon fibres, the mechanical properties of SSWM are rather ductile and highly nonlinear after the yielding point. The advantages of SSWM are : High tensile strength, high modulus of elasticity, low weight, corrosion resistance, minimum change in column geometry, rapid installation process, high ductility, and cost effective . In this investigation, locally available stainless steel wire mesh (SSWM) has been used as the wrapping material for confinement of concrete columns for axial strength enhancement.

Experimental methods for evaluating the increase in axial strength of columns are laborious, time consuming, difficult and costly. So numerical methods are best suited to study the effect of SSWM wraps on axial strength of columns. The performance of the structural elements can be predicted and analysed with greater accuracy by Finite Element Analysis (FEA) compared to experimental approach. For concrete structures, FEA is widely used numerical method. The objective of the present study is to implement the nonlinear FE modelling and analysis to evaluate the axial load carrying capacity of control and SSWM wrapped plain cement concrete (PCC) and reinforced cement concrete (RCC) columns.

The performance evaluation of SSWM wrapped structural elements is less explored research area, so strengthening of circular columns with SSWM needs to be investigated. Nonlinear FE analysis is very useful for determining internal stress distribution and load carrying capacity of structural elements. With the use of FE software, the increase in axial load carrying capacity and behaviour of the SSWM wrapped columns is evaluated and presented in this paper.

2. Literature review

Literature review has been carried out for concrete damage plasticity model, bond behaviour, axial strengthening of FRP wrapped column for numerical and analytical studies. Obaidat, Heyden *et al.* (2010) presented a FE analysis of eight beams having same rectangular cross section. The beams were loaded under four point bending. ABAQUS tool was used for numerical analysis. A

plastic damage model was used for the concrete. The stress strain relationship developed by Saenz (1964) was used for concrete under uniaxial compression. Perfect bond between steel and concrete was considered for analysis. 4-node tetrahedral meshing was used for concrete and steel plates. Two models for CFRP were used for study. The first model was considered as linear elastic isotropic and other model was considered as linear elastic orthotropic. Two methods used for interface between concrete and CFRP. The first one was considered as perfect bond and other model was considered as cohesive bond. Four types of model for each CFRP retrofitted beams were considered. Cohesive bond model showed good result compared to perfect bond. There was very little effect of orthotropic and isotropic material. But based upon analysis orthotropic material was considered best suited for analysis. The analysis result showed good agreement with the experimental data regarding load-displacement response. Massicotte, Elwi *et al.* (1990) developed the tension-softening behaviour of plain concrete and reinforced concrete structures. Depending upon the fracture energy, post-cracking stress strain curve of concrete in tension was proposed. For determining stress strain relationship of concrete under tension, two parameters were calculated one was fracture energy and the other was average crack strain. Perfect bond between concrete and reinforcement was assumed. The stress strain relationship for concrete in tension was verified against various types of structural elements and under different loading conditions. Hu, Lin *et al.* (2010) performed nonlinear finite element analysis of reinforced concrete and prestressed concrete structure strengthened by FRP. The stress-strain relationship of Saenz has been adopted for concrete in compression. Tension stiffening curve for concrete in tension was used. For numerical analysis, ABAQUS was used for nonlinear finite element analysis. The analysis result showed good agreement for columns, beam etc. with experimental result. Tao and Chen (2014) presented finite element model for simulating the bond behaviour between concrete and FRP. Concrete damage plasticity model was used for the concrete modelling. The concrete was modelled using square elements with four integration points (CPS4). Four type of meshing for concrete were considered with size equal to 5 mm, 2 mm, 1 mm, 0.5 mm. As mesh size increased load carrying capacity increased slightly. The analysis result showed good agreement with the experimental data regarding load-displacement. Allam, Shoukry *et al.* (2013) presented finite element analysis of control beams tested by Managat and Elgarf. Stress strain relationship for concrete in compression was considered from Egyptians Code ECP-203. Concrete was modelled using 8 node solid elements. Steel reinforcement was modelled as 3-D, 2 node truss elements. Perfect bond was assumed between concrete and steel. Smearred crack approach was used for concrete. Steel was modelled as linear elastic-perfectly plastic. Stress strain relationship of concrete in tension was modelled using Massicotte, Elwi *et al.* (1990). Gambarelli, Nistico *et al.* (2014) presented finite element modelling of concrete columns confined with CFRP. Behaviour of columns wrapped with CFRP depended on interaction between mechanical properties and dilation angle of concrete. CFRP wrapped column was modelled as concrete plus epoxy plus fibres as shown in Fig. 2. The finite element analysis of concrete confined column was carried out by 3D FE program MASA. The uniaxial stress strain curves were presented and compared with the experimental results. Typical failure mode of the model was presented and was similar to the experiment failure. Effect of the FRP jackets was more in circular section column than other column cross-section. From the result, CFRP in non-circular sections had non-uniform compressive stress distribution. Failure of the column was due to tensile failure of CFRP and the failure was brittle.

Turon, Davila *et al.* (2007) presented a methodology to determine the constitutive parameters for the simulation of progressive delamination. The procedure accounted for the size of a cohesive finite element and the length of the cohesive zone to ensure the correct dissipation of energy. In

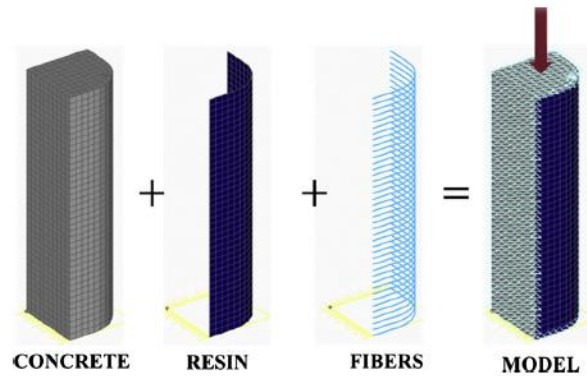


Fig. 2 Modelling of Concrete, Epoxy and FRP

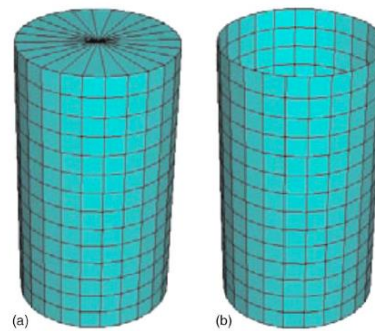


Fig. 3 FRP to concrete modelling

addition, a closed-form expression for estimating the minimum penalty stiffness necessary for the constitutive equation of a cohesive finite element was presented. The resulting constitutive law allowed the use of coarser finite element meshes than was usually admissible, which rendered the analysis of large-scale progressive delamination problems computationally tractable. Coronado and Lopez (2007) described numerical study of structural behaviour of concrete strengthened with FRP sheets or plates. FE software ABAQUS was used for numerical analysis. FRP modelled as CPE4R (plain strain elements with reduced integration). Tie constraint was used for connecting meshes of different material. Finite element analysis showed good agreement in terms of load displacement, failure pattern and post failure behaviour with experimental result. Karabinis, Rousakis *et al.* (2008) performed numerical analysis of column confined with fiber reinforced polymer sheet. Finite element software ABAQUS was used. Concrete was modelled as Drucker-Prager type material. Eight-node solid element (C3D8R) was used. Behaviour of steel was assumed as inelastic behaviour and eight-node solid element was used for analysis as shown in Fig. 3. Behaviour of FRP was considered orthotropic linearly elastic up to failure and modelled as quadrilateral lamina element with membrane properties (M3D4R). FE analysis of circular columns confined by one, two or three wrappings of carbon fiber was carried out as well as square column of 200 mm cross section with corner radius of 30 mm. Monotonic axial load was imposed concentrically on concrete surface. Stress strain curve obtained from FE analysis have been presented. Hu and Barbato (2014) studied finite element analysis of reinforced concrete (RC)

circular columns confined with externally-bonded fiber-reinforced polymers. A two-node one-dimensional force-based frame finite element analysis was carried out. One dimensional nonlinear constitutive model was employed to describe the stress-strain behaviour of unconfined, steel-confined, and FRP-confined concrete. From FE analysis the ultimate load-carrying capacity of FRP-confined RC columns and load displacement response subjected to concentric axial load were found out and which showed good agreement with experimental results. Rocca, Galati *et al.* (2008) compared four different guidelines for the strengthening of reinforced concrete columns of both circular and prismatic cross sections by means of fiber-reinforced polymer (FRP) confinement and Ozbakkaloglu, Lim *et al.* (2013) reviewed 88 models developed to predict the axial stress-strain behaviour of FRP-confined concrete and confinement strength in circular sections. Models were divided into two parts: design oriented models and analysis oriented models. From the comparison design oriented models performed better than analysis oriented model. Hu (2013) presented assessment result of existing criteria for fiber reinforced polymer (FRP) confined concrete and proposed an improved criterion. Both circular and rectangular columns were reviewed. From analysis, existing criteria for circular column was found better than the existing criteria of rectangular column.

3. Finite element modelling

ABAQUS is used for general purpose finite element modelling (FEM) and analysis. It is useful for complete solutions for linear and nonlinear problems. In general Finite element software (ABAQUS) consists of following three steps (ABAQUS User’s manual)

Four node linear tetrahedral element is used for 3D modelling of concrete. This element has 4 nodes with six degree of freedom on each node i.e., three translation degree and three rotational



Fig. 4 Principle steps in ABAQUS

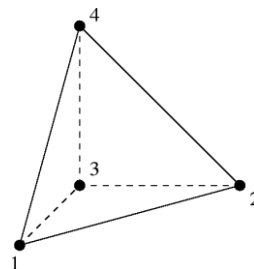


Fig. 5 Four node linear tetrahedral element

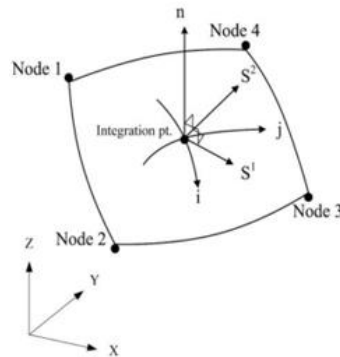


Fig. 6 S4R element (Zare and Janghorban 2013)

degrees. This element is capable of crushing, cracking and plastic deformation. Tetrahedral element is versatile and mostly used for automatic meshing. Different size of element 50 mm×50 mm×50 mm, 25 mm×25 mm×25 mm, 12.5 mm×12.5 mm×12.5 mm are considered for analysis. The Fig. 5 shows 4 node tetrahedral element. Steel reinforcement is modelled with 2-node linear 3-D truss type of elements.

Four nodes doubly curved thin or thick shell, reduced integration, hourglass control, finite membrane strains is used for modelling SSWM. In S4R, S means conventional stress/displacement shell, 4 are number of nodes, and R means reduced integration.

3.1 Material properties

The material properties of concrete, reinforcement and SSWM used for numerical modelling are discussed in the following sub-sections:

3.1.1 Concrete

Concrete is defined as an isotropic material before yielding and cracking model is defined for nonlinear analysis. The density of concrete is taken as 2400 kg/m³. The poisson's ratio of concrete is 0.2 based on literature. Modulus of elasticity is defined according to IS: 456 (2000) as shown in Eq. (1).

$$E = 5000 \times \sqrt{f_{ck}} \quad (1)$$

Where, f_{ck} is unconfined compressive strength of concrete grade under consideration. To predict the behaviour of concrete, non-linear analysis is carried out. Two methods are available in ABAQUS viz Smeared crack model and concrete damage plasticity. Concrete damage plasticity is selected for non-linear analysis because it has higher potential for convergence as compared to smeared crack model. The concrete damage plasticity model uses concepts of isotropic damage elasticity in conjunction with isotropic tensile and compressive plasticity to represent the inelastic behaviour of concrete. The concrete damaged plasticity model uses stress v/s strain relationships to correlate parameters for relative concrete damage for both tension and compression. In addition to these basic parameters that identify stress vs strain relationships, parameters based upon the microstructure of concrete must also be identified. For the purpose of this finite element model, these parameter include dilation angle (ϕ), plastic potential eccentricity (e), initial biaxial/uniaxial

ratio (f_{bo}/f_{co}), the shape of the loading surface (Kc) and viscosity parameter. These parameters are described as under-

Dilation angle (ϕ): It is concrete internal friction angle. For numerical simulations, the value of dilation angle is assumed as 37 degrees.

Plastic potential eccentricity (e): It is the ratio between tensile and compressive strength of concrete. For numerical simulations default value of 0.1 is taken (ABAQUS User’s manual).

Initial biaxial/uniaxial ratio (f_{bo}/f_{co}): It is the ratio between the initial biaxial compressive yield stress and the initial uniaxial compressive yield stress, which is taken as 1.16 (ABAQUS User’s manual).

Shape of the loading surface (Kc): It describes the ratio of the distance between the hydrostatic axis and the compression meridian and the tension meridian in the deviatoric cross section, respectively. For numerical simulation a value of 2/3 is recommended in ABAQUS manual (ABAQUS User’s manual).

Viscosity parameter: It is taken as zero for the numerical simulation.

The stress –strain relationship proposed by Saenz (1964) is used for uniaxial compressive stress-strain curve for concrete as shown in Fig. 7. This relation is derived using equations 2,3 and 4 given below-

$$\sigma_c = \frac{E_c \times \epsilon_c}{1 + (R + R_E - 2) \left(\frac{\epsilon_c}{\epsilon_0}\right) - (2R - 1) \left(\frac{\epsilon_c}{\epsilon_0}\right)^2 + R \left(\frac{\epsilon_c}{\epsilon_0}\right)^3} \tag{2}$$

$$\text{Where } R = \frac{R_E (R_\sigma - 1)}{(R_E - 1)^2} - \frac{1}{R_E} \tag{3}$$

$$\text{Modular Ratio; } R_E = \frac{E_c}{E_0} \tag{4}$$

σ_c = Stress in concrete

ϵ_c = Strain in concrete

E_c = Initial modulus of elasticity

f'_c = maximum compressive strength of concrete.

Strain ratio ; $R_E = \epsilon_f / \epsilon_0$

Stress ratio ; $R_\sigma = f'_c / \sigma_f$

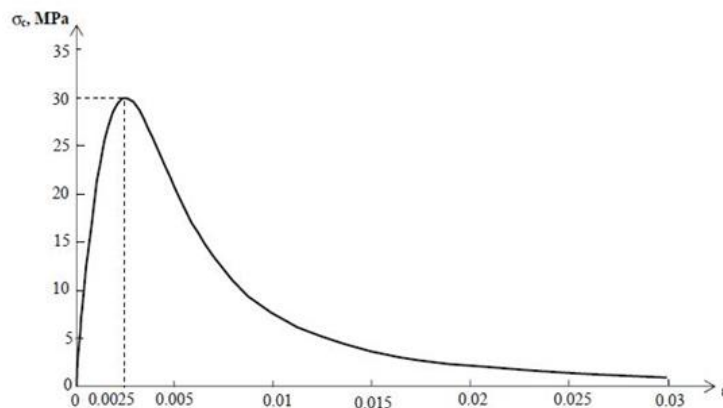


Fig. 7 Stress-strain relationship of concrete under uniaxial compression (Saenz 1964)

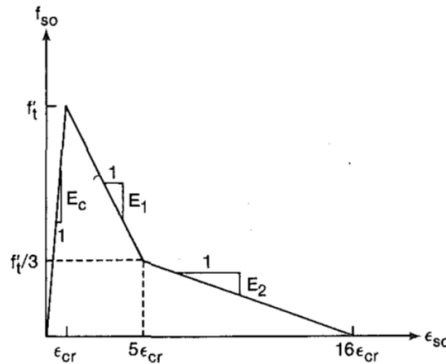


Fig. 8 Stress-strain relationship of concrete under uniaxial tension (Massicotte, Elwi *et al.* 1990)

ϵ_f and σ_f are maximum strain and corresponding stress on the uniaxial stress-strain curve.

ϵ_0 = strain corresponding to f'_c in an uniaxial compressive test = 0.0025.

Secant modulus; $E_0 = \frac{f'_c}{\epsilon_0}$,

$R_\epsilon = 4$, $R_\sigma = 4$

The stress strain relationship proposed by Massicotte, Elwi *et al.* (1990) is used for uniaxial tensile stress strain curve for concrete in tension as shown in Fig. 8. It is a trilinear stress-strain curve with a linear ascending branch and a bilinear softening branch for concrete after cracking. The notations used are:

E_c = initial tangent modulus of elasticity of concrete.

E_1, E_2 = Tangent modulus in concrete softening branch

f_{so} = concrete stress due to tension softening.

f'_t = uniaxial tensile strength of concrete.

ϵ_c = concrete strain due to tension softening

ϵ_{cr} = strain in concrete at cracking

f'_c = compressive strength of concrete

3.1.2 Steel reinforcement

The Stress-strain relationship of Fe 415 is taken from IRC 112 (2011) and is shown in Fig. 9. Plasticity is defined as stress vs plastic strain relationship. The initial value of plastic strain is taken as zero for analysis.

3.1.3 Stainless steel wire mesh (SSWM)

SSWM is an isotropic material. Tensile strength test has been carried out on three samples of SSWM for finding the tensile properties of SSWM in laboratory (Kumar and Patel 2016). Based upon the tensile test, Young's modulus comes out to be 151GPa. Poisson's ratio is assumed to be 0.3. For nonlinear properties, stress-strain relationship of SSWM as found experimentally is shown in Fig. 10.

3.2 Numerical modelling

Nonlinear finite element (FE) analysis of control specimen and SSWM wrapped PCC and RCC

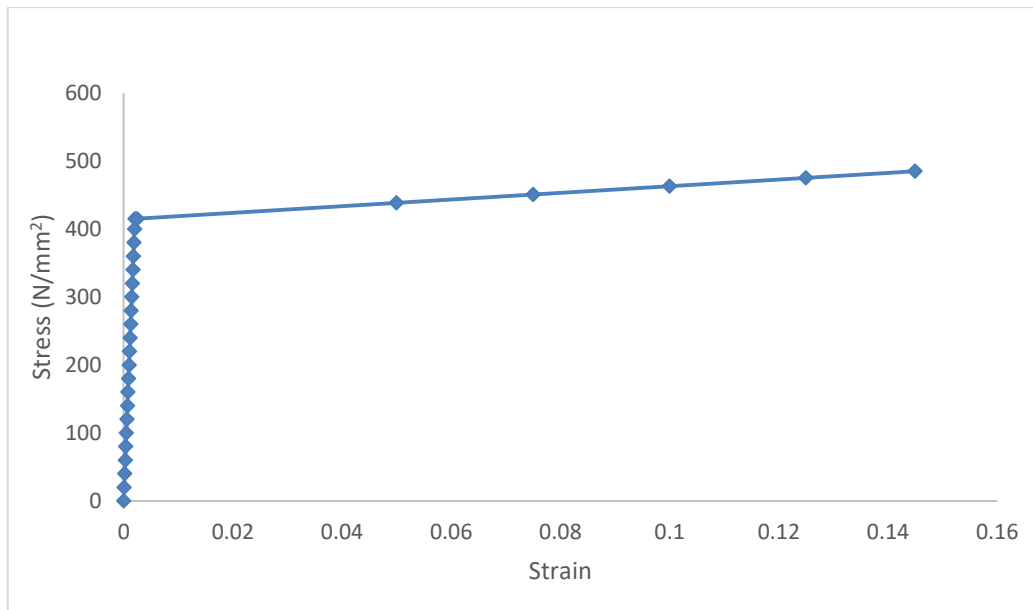


Fig. 9 Stress-strain relationship of Fe 415 steel (IRC:112 2011)

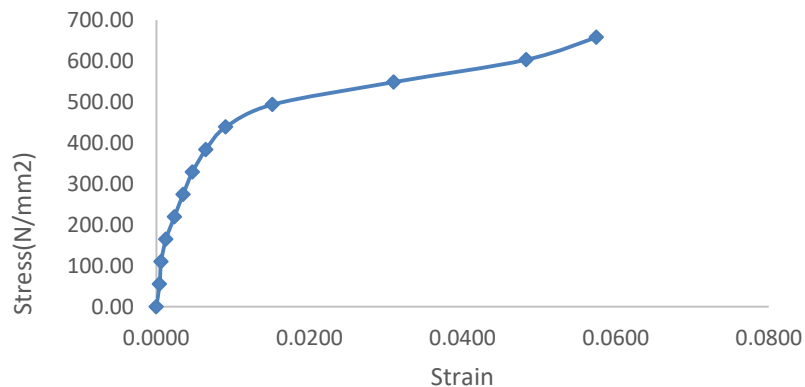


Fig. 10 Stress-strain relationship of SSWM (Kumar and Patel 2016)

circular columns has been carried out using FE software ABAQUS. All columns have the same cross-sectional dimension but with variable heights and are subjected to uniaxial compressive loading. The analysis has been carried by modelling columns with one wrap and two wraps of SSWM so as to find the increase in the load carrying capacity for increase in no. of wraps. PCC columns of 200 mm diameter and height 400 mm, 800 mm, and 1200 mm are considered. The RCC columns of 200 mm diameter and 1200 mm height are considered and shown in Fig. 11. Three different grades of concrete M15, M20 and M25 are considered for analysis.

Fe 415 grade of steel with density as 7810 kg/m^3 , Modulus of elasticity 200 GPa and Poisson's ratio 0.3 is used for analysis. For nonlinear properties, stress strain relationship of steel as given in IRC 112 (2011) is used and shown in Table 1. For RCC columns of 1200 mm height, the main

Table 1 Stress strain relationship of steel

| Sr no. | Stress (N/mm ²) | Strain |
|--------|-----------------------------|--------|
| 1 | 415.00 | 0 |
| 2 | 438.47 | 0.050 |
| 3 | 450.71 | 0.075 |
| 4 | 462.96 | 0.100 |
| 5 | 475.20 | 0.125 |
| 6 | 485.00 | 0.145 |

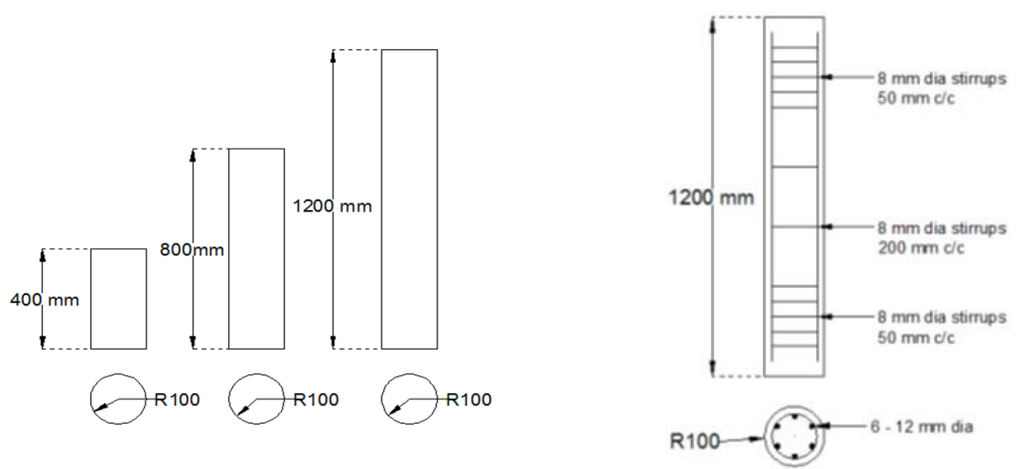


Fig. 11 Geometry of PCC and RCC columns

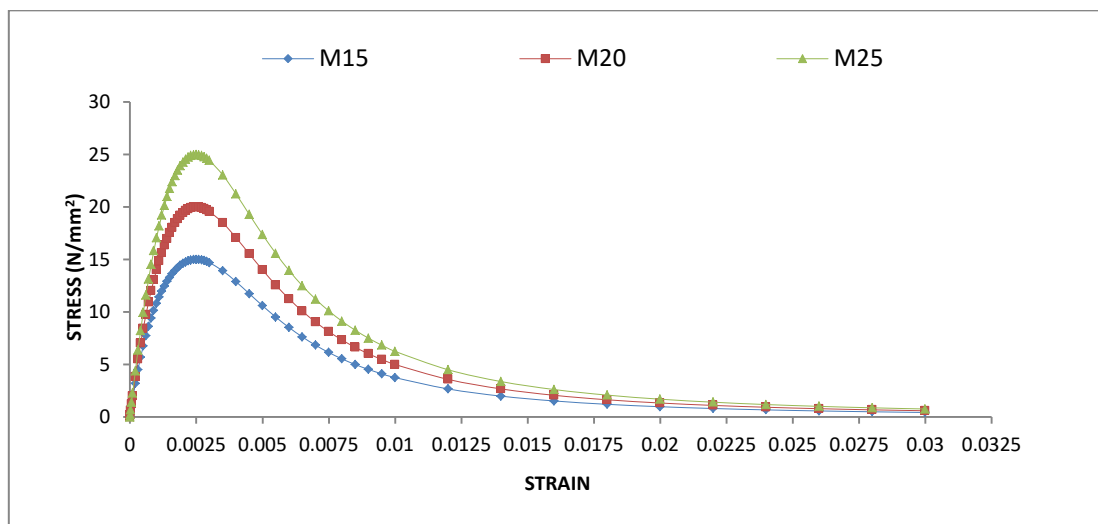


Fig. 12 Compressive behaviour of concrete

reinforcement is taken as 6 bars of 12mm diameter and transverse reinforcement consists of 8 mm dia at 50 mm c/c spacing at top and bottom up to distance 250 mm each. For the middle height of

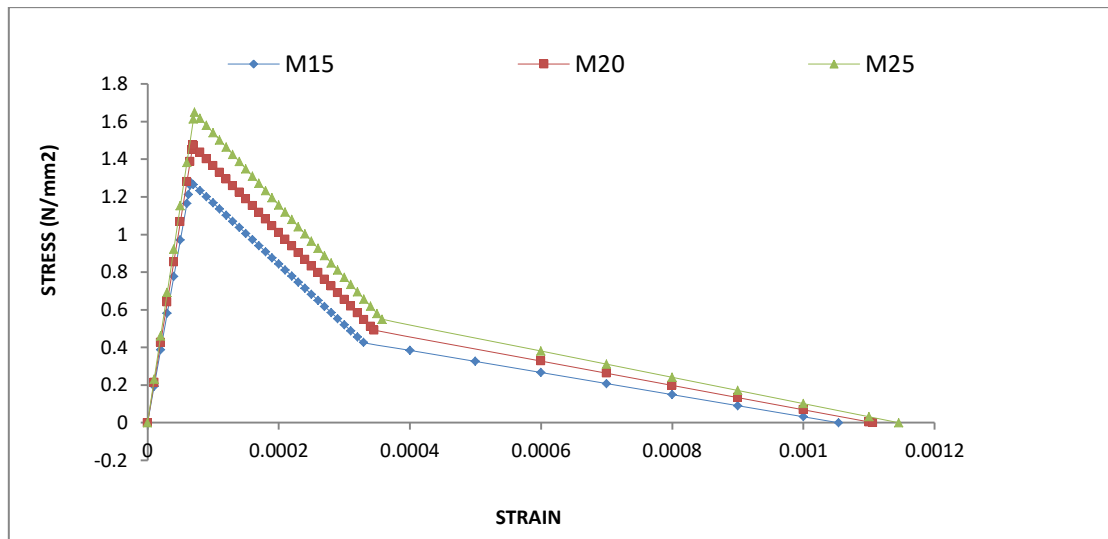


Fig. 13 Tensile behaviour of concrete

column, the stirrup spacing is kept 200 mm c/c and is shown in Fig. 11.

The stress- strain relationship for uniaxial compression is found using relationship proposed by Saenz (1964) and are shown in Fig. 12. This relation is derived using equations 2,3 and 4. The stress- strain relationship for concrete under uniaxial tension is taken from Massicotte (1990) for different grades of concrete and are shown in Fig. 13.

For SSWM, shell homogenous section is created and their respective properties are assigned to it. Thickness of SSWM is taken as 0.25 mm. Two different models can be used to represent the interface between concrete and SSWM. In the first model, the interface can be modelled as a perfect bond while in the second it can be modelled using a cohesive zone model. Both ABAQUS/Standard and ABAQUS/Explicit allow modelling of progressive damage and failure in cohesive wrappings whose response is defined in terms of traction-separation. This general framework allows the combination of several damage mechanisms acting simultaneously on the same material. Each failure mechanism consists of three ingredients: a damage initiation criterion, a damage evolution law, and a choice of element removal (or deletion) upon reaching a completely damaged state. While this general framework is same for traction-separation response and conventional materials, many details to define various ingredients are different. Therefore, the details of damage modelling for traction-separation response are presented below.

For SSWM and concrete, perfect bonding is assumed in current study. For perfect bonding, tie constraint is used. In perfect bonding there is no translation between SSWM and concrete. For tie constraint, concrete is selected as a master surface and SSWM is selected as slave surface. For two wraps of SSWM, inner wrap which is connected to the concrete is considered as master surface and outer wrap is considered as slave surface. Column is tested under uniaxial compressive. For uniaxial compression loading, load is applied on the top of the column. Pinned condition is applied for boundary conditions at the bottom of the column as shown in Fig. 14, numerical model of concrete steel and SSWM is shown in Fig. 15. For this study three different type of meshing size 50 mm, 25 mm and 12.5 mm as shown in Fig. 16 is adopted.

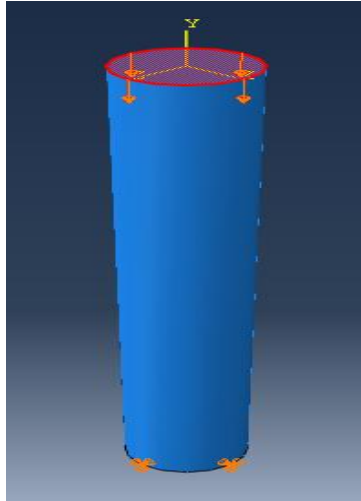


Fig. 14 Loading and boundary condition

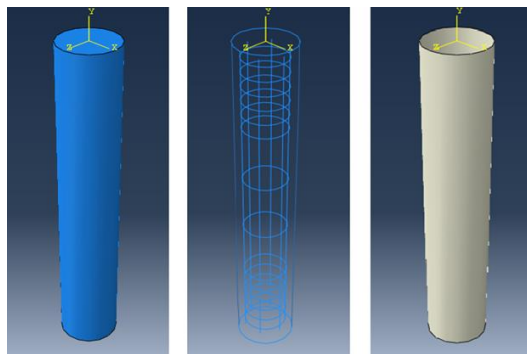


Fig. 15 Concrete, reinforcement and SSWM model in ABAQUS

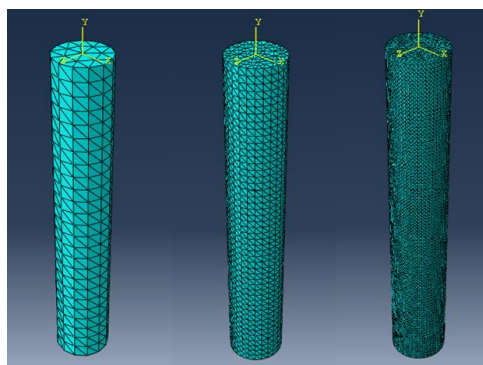


Fig.16 Mesh elements

4. Notation for columns

Notation for different columns with different heights and mesh size are described in Table 2. In

Table 2 Notation for columns

| Sr no. | Column | Concrete grade | Type of column | Height of column (mm) | Mesh size (mm) |
|--------|---------|----------------|----------------|-----------------------|----------------|
| 1 | M15P4F | M15 | PCC | 400 | 12.5 |
| 2 | M15P4M | M15 | PCC | 400 | 25 |
| 3 | M15P4C | M15 | PCC | 400 | 50 |
| 4 | M15P8F | M15 | PCC | 800 | 12.5 |
| 5 | M15P8M | M15 | PCC | 800 | 25 |
| 6 | M15P8C | M15 | PCC | 800 | 50 |
| 7 | M15P12F | M15 | PCC | 1200 | 12.5 |
| 8 | M15P12M | M15 | PCC | 1200 | 25 |
| 9 | M15P12C | M15 | PCC | 1200 | 50 |
| 10 | M15R12F | M15 | RCC | 1200 | 12.5 |
| 11 | M15R12M | M15 | RCC | 1200 | 25 |
| 12 | M15R12C | M15 | RCC | 1200 | 50 |
| 13 | M20P4F | M20 | PCC | 400 | 12.5 |
| 14 | M20P4M | M20 | PCC | 400 | 25 |
| 15 | M20P4C | M20 | PCC | 400 | 50 |
| 16 | M20P8F | M20 | PCC | 800 | 12.5 |
| 17 | M20P8M | M20 | PCC | 800 | 25 |
| 18 | M20P8C | M20 | PCC | 800 | 50 |
| 19 | M20P12F | M20 | PCC | 1200 | 12.5 |
| 20 | M20P12M | M20 | PCC | 1200 | 25 |
| 21 | M20P12C | M20 | PCC | 1200 | 50 |
| 22 | M20R12F | M20 | RCC | 1200 | 12.5 |
| 23 | M20R12M | M20 | RCC | 1200 | 25 |
| 24 | M25R12C | M20 | RCC | 1200 | 50 |
| 25 | M25P4F | M25 | PCC | 400 | 12.5 |
| 26 | M25P4M | M25 | PCC | 400 | 25 |
| 27 | M25P4C | M25 | PCC | 400 | 50 |
| 28 | M25P8F | M25 | PCC | 800 | 12.5 |
| 29 | M25P8M | M25 | PCC | 800 | 25 |
| 30 | M25P8C | M25 | PCC | 800 | 50 |
| 31 | M25P12F | M25 | PCC | 1200 | 12.5 |
| 32 | M25P12M | M25 | PCC | 1200 | 25 |
| 33 | M25R12C | M25 | PCC | 1200 | 50 |
| 34 | M25R12F | M25 | RCC | 1200 | 12.5 |
| 35 | M25R12M | M25 | RCC | 1200 | 25 |
| 36 | M25R12C | M25 | RCC | 1200 | 50 |

column notations first three terms represent concrete grade M15/M20/M25 having characteristic compressive strength $15 \text{ N/mm}^2/20 \text{ N/mm}^2/25 \text{ N/mm}^2$ respectively, fourth term P or R represents plain concrete or reinforced concrete. Fifth term 4/8/12 represents 400 mm/800 mm/1200 mm height of columns. Last term F, M, C indicates fine, medium or coarser finite element mesh size.

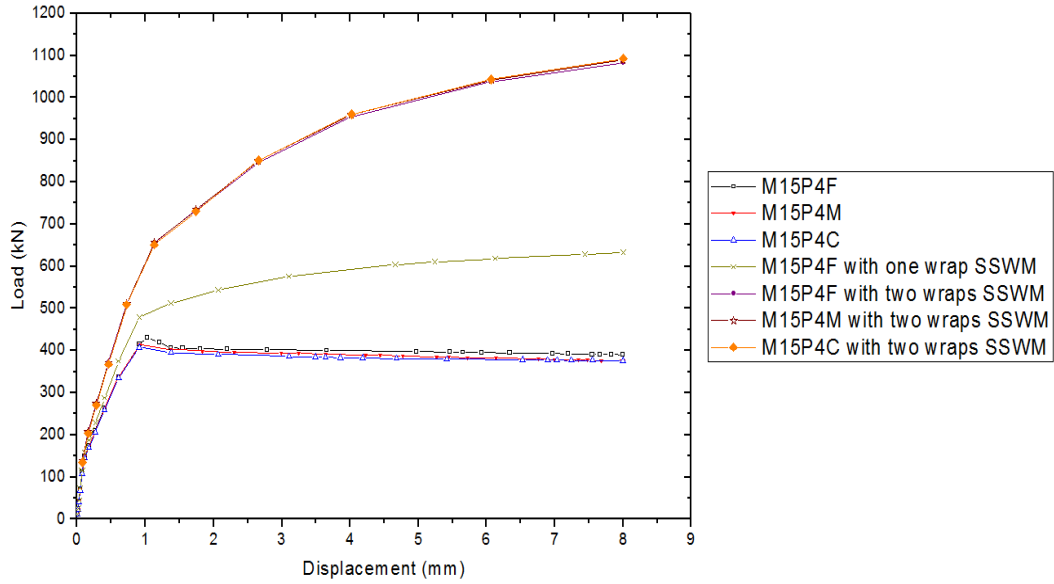


Fig. 17 M15 PCC column with height 400 mm

Table 3 Comparison of ultimate axial load capacity of PCC columns from numerical analysis and experimental investigations

| Concrete grade | Height of column (mm) | No. of wraps | NUMERICAL ANALYSIS | | EXPERIMENTAL WORK | | ALC _{Num} / ALC _{Exp} |
|----------------|-----------------------|--------------|---------------------------------------|---------------------|---------------------------------------|---------------------|---|
| | | | Axial load carrying capacity (ALC) kN | Percentage increase | Axial load carrying capacity (ALC) kN | Percentage increase | |
| M 15 | 400 | 0 | 430 | | 530 | | 0.81 |
| | | 1 | 632 | 46.98 | 630 | 18.87 | 1.00 |
| | | 2 | 1092 | 153.95 | 790 | 49.06 | 1.38 |
| | 800 | 0 | 431 | | 485 | | 0.89 |
| | | 1 | 591 | 37.12 | 780 | 60.82 | 0.76 |
| | | 2 | 946 | 119.49 | 830 | 71.13 | 1.14 |
| | 1200 | 0 | 410 | | 500 | | 0.82 |
| | | 1 | 560 | 36.59 | 805 | 61.00 | 0.70 |
| | | 2 | 830 | 102.44 | 930 | 86.00 | 0.89 |
| M-20 | 400 | 0 | 561 | | 620 | | 0.90 |
| | | 1 | 771 | 37.43 | 715 | 15.32 | 1.08 |
| | | 2 | 1235 | 120.14 | 910 | 46.77 | 1.36 |
| | 800 | 0 | 563 | | 660 | | 0.85 |
| | | 1 | 735 | 30.55 | 970 | 46.97 | 0.76 |
| | | 2 | 1092 | 93.96 | 1105 | 67.42 | 0.99 |
| | 1200 | 0 | 580 | | 610 | | 0.95 |
| | | 1 | 671 | 15.69 | 940 | 54.10 | 0.71 |
| | | 2 | 981 | 69.14 | 1040 | 70.49 | 0.94 |

Table 3 Continued

| | | | | | | | |
|------|------|---|------|--------|------|-------|------|
| | | 0 | 675 | | 800 | | 0.84 |
| | 400 | 1 | 889 | 31.70 | 920 | 15.00 | 0.97 |
| | | 2 | 1381 | 104.59 | 1110 | 38.75 | 1.24 |
| M-25 | 800 | 0 | 729 | | 810 | | 0.90 |
| | | 1 | 871 | 19.48 | 1050 | 29.63 | 0.83 |
| | | 2 | 1237 | 69.68 | 1230 | 51.85 | 1.01 |
| | 1200 | 0 | 726 | | 790 | | 0.92 |
| | | 1 | 848 | 16.80 | 1060 | 34.18 | 0.80 |
| | | 2 | 1119 | 54.13 | 1240 | 56.96 | 0.90 |

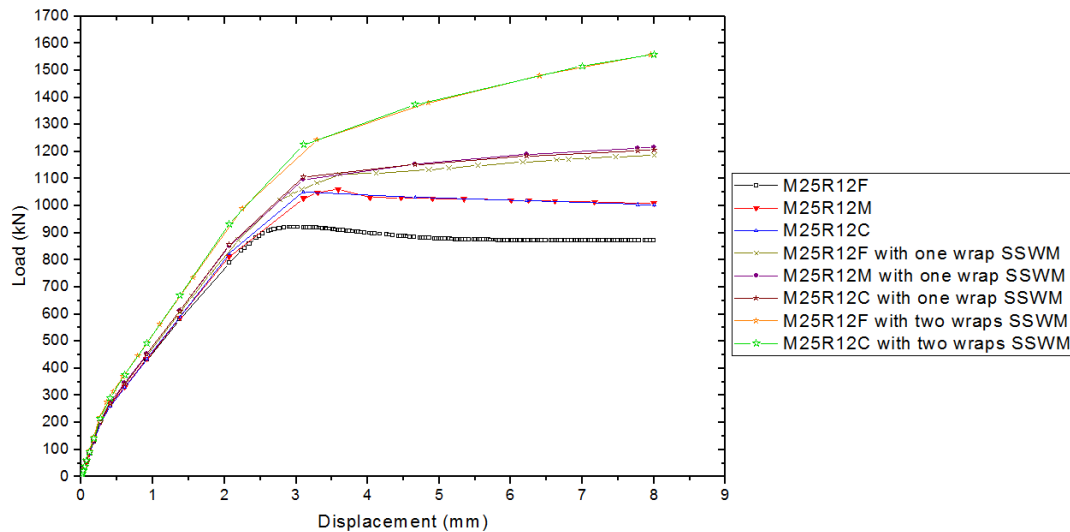


Fig. 18 M25 RCC column with height 1200 mm

5. Results

From the nonlinear FE analysis of columns with and without SSWM wraps, load-displacement curves are obtained. The load vs displacement curve for M15 grade PCC column of 400 mm height is shown in Fig. 17. It is observed that the ultimate load is 430 kN, 632 kN and 1092 kN for control PCC column, singly wrapped and doubly wrapped columns with SSWM respectively. From Fig. 17, it is observed that mesh size is not affecting the results significantly. So for comparison of load carrying capacity of column, 25 mm mesh is considered. The comparison of load carrying capacity of SSWM wrapped PCC columns with different number of wraps and control PCC columns are summarised in Table 3. Experimental Investigation of SSWM wrapped PCC circular columns to evaluate increase in axial load capacity has been carried out by authors (Kumar and Patel 2016). The results obtained from numerical simulation and experimental investigation are also presented in Table 3. Load displacement curve for M15 grade concrete PCC columns of 400 mm, 800 mm and 1200 mm with and without SSWM wrapping, as obtained from experimental investigation and numerical simulation, are presented in Figs. 19, 20 and 21

Table 4 Ultimate axial load capacity for RCC columns from numerical analysis

| Concrete grade | No. of wraps | Height of column (mm) | Ultimate load carrying capacity of column (kN) | | |
|----------------|--------------|-----------------------|--|----------------|---------------------|
| | | | Axial strength | % age increase | % relative increase |
| M15 | 0 | 1200 | 752 | | |
| | 1 | 1200 | 936 | 24.47 | |
| | 2 | 1200 | 1285 | 70.87 | 189.61 |
| M20 | 0 | 1200 | 910 | | |
| | 1 | 1200 | 1077 | 18.35 | |
| | 2 | 1200 | 1417 | 55.71 | 203.59 |
| M25 | 0 | 1200 | 1067 | | |
| | 1 | 1200 | 1216 | 13.96 | |
| | 2 | 1200 | 1571 | 47.23 | 238.32 |

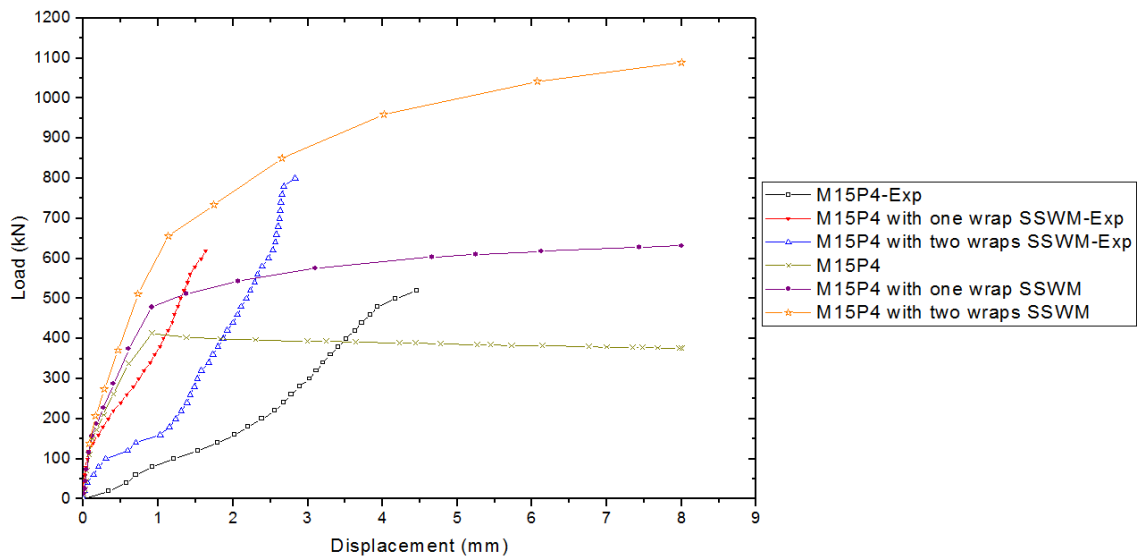


Fig. 19 Comparison of M15 grade PCC column with height 400 mm

respectively.

Load vs displacement curve for M25 grade reinforced concrete (RCC) column of 1200 mm height is shown in Fig. 18. It is observed that the ultimate load is 1067 kN, 1216 kN and 1571 kN for control column, singly wrapped and doubly wrapped columns with SSWM respectively. The comparison of load carrying capacity of SSWM wrapped RCC columns of 1200 mm height with different number of wraps and control RCC columns are summarised in Table 4.

There are various design codes and guidelines available for finding load carrying capacity of CFRP and GFRP strengthened columns like ACI 440.2R-08 (2008) and CNR-DT 200/2004 (2004) but so far, no such guidelines exists for SSWM wrapped columns. However an attempt has been made to use ACI 440.2R-08 and CNR-DT 200/2004 guidelines for finding the ultimate load carrying capacity of SSWM wrapped circular column. The comparison of axial load carrying

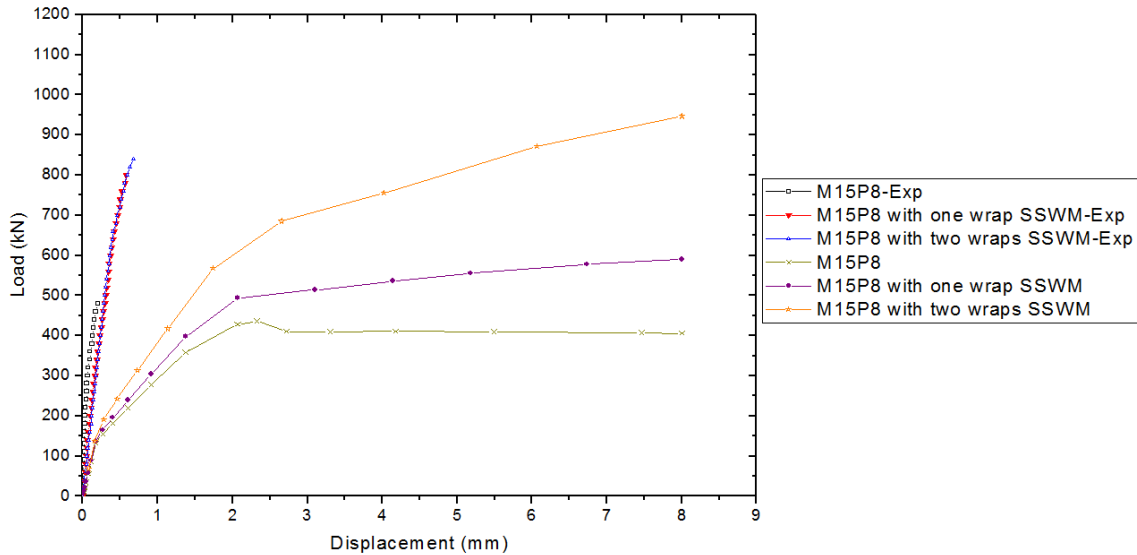


Fig. 20 Comparison of M15 grade PCC column with height 800 mm

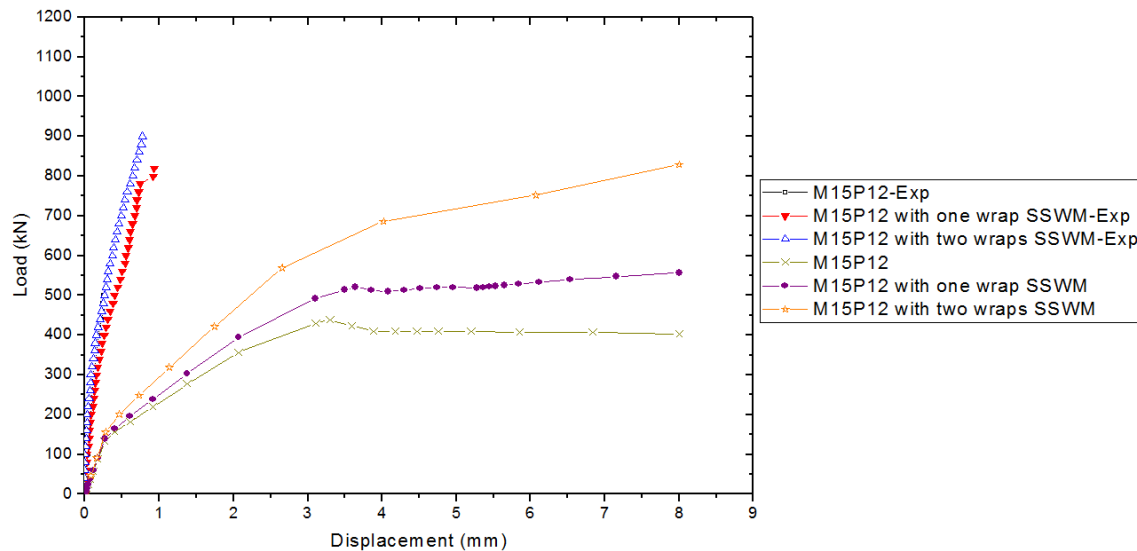


Fig. 21 Comparison of M15 grade PCC column with height 1200 mm

capacity based on design guidelines and numerical simulation is presented in Table 5. ACI440.2R-08 and CNR-DT 200/2004 guidelines are given for short columns and so axial load carrying capacity of 400mm, 800 mm and 1200 mm height of PCC columns is same. For comparison purposes average increase of axial load carrying capacity obtained from numerical simulation of various heights is considered. The percentage increase in axial load capacities by numerical simulation, ACI 440.2R, CNR DT/200 and experimental work are presented in Table no. 6

Table 5 Comparison of axial load capacity of columns from numerical and analytical analysis

| Grade of concrete | No. of SSWM wraps | Axial Load Capacity (ALC) | | | | ACI 440 2R 2008 (kN) | CNR DT 200/ 2004 (kN) | Ratio of ALC by numerical analysis and ACI 2R | Ratio of ALC by numerical analysis and CNR DT |
|-------------------|-------------------|---------------------------|--------|---------|--------------------|----------------------|-----------------------|---|---|
| | | Numerical analysis | | | | | | | |
| | | 400 mm | 800 mm | 1200 mm | Avg. strength (kN) | | | | |
| M 15 | 0 | 430 | 431 | 410 | 423.67 | 471 | 471 | 0.90 | 0.90 |
| | 1 | 632 | 591 | 560 | 594.33 | 688 | 683 | 0.86 | 0.87 |
| | 2 | 1092 | 946 | 830 | 956.00 | 1168 | 832 | 0.82 | 1.15 |
| M 20 | 0 | 561 | 563 | 580 | 568.00 | 628 | 628 | 0.90 | 0.90 |
| | 1 | 771 | 735 | 671 | 725.67 | 758 | 851 | 0.96 | 0.85 |
| | 2 | 1235 | 1092 | 981 | 1102.67 | 1237 | 1015 | 0.89 | 1.09 |
| M 25 | 0 | 675 | 729 | 726 | 710.00 | 785 | 785 | 0.90 | 0.90 |
| | 1 | 889 | 871 | 848 | 869.33 | 827 | 1015 | 1.05 | 0.86 |
| | 2 | 1381 | 1237 | 1119 | 1245.67 | 1307 | 1192 | 0.95 | 1.05 |

Table 6 Comparison of percentage increase axial load capacity of PCC columns obtained from Numerical and Analytical work

| Grade of Concrete | No. of wraps | Axial load capacity (kN) | | | | Percentage increase in axial capacity | | | |
|-------------------|--------------|----------------------------------|---------|--------|-------------------------------------|---------------------------------------|---------|--------|-------------------|
| | | Num. Ana.(avg. of three heights) | ACI 440 | CNR-DT | Exp. Result (avg. of three heights) | Num. Ana. | ACI 440 | CNR-DT | Exp. Result (Avg) |
| | | | | | | | | | |
| M15 | 0 | 424 | 471 | 471 | 505 | - | - | - | - |
| | 1 | 594 | 688 | 683 | 738 | 40.09 | 46.07 | 45.01 | 46.72 |
| | 2 | 956 | 1168 | 832 | 850 | 125.47 | 147.98 | 76.65 | 68.99 |
| M20 | 0 | 568 | 628 | 628 | 630 | - | - | - | - |
| | 1 | 726 | 758 | 851 | 875 | 27.82 | 20.70 | 35.51 | 38.89 |
| | 2 | 1103 | 1237 | 1015 | 1018 | 94.19 | 96.97 | 61.62 | 61.58 |
| M25 | 0 | 710 | 785 | 785 | 800 | - | - | - | - |
| | 1 | 869 | 827 | 1015 | 1010 | 22.39 | 5.35 | 29.30 | 26.25 |
| | 2 | 1246 | 1307 | 1192 | 1193 | 75.49 | 66.50 | 51.85 | 49.12 |

6. Discussions

1. As per numerical analysis, the increase in load carrying capacity of 400mm height of columns with one wrapping of SSWM is 46.98%, 37.43% and 31.70% for M15, M20 and M25 grade concrete columns respectively. With two wrapping, it is 153.95%, 120.14% and 104.59%. The increase in load carrying capacity of 800mm height columns with one wrapping of SSWM is 37.12%, 30.55% and 19.48% for M15, M20 and M25 grade concrete columns respectively. With two wrapping, it is 119.49%, 93.96% and 69.68%. The increase in load carrying capacity of 1200 mm height of columns with one wrapping of SSWM is 36.59%, 15.69% and 16.80% for M15, M20 and M25 grade concrete columns respectively. With two

wrapping, it is 102.44%, 69.14% and 54.13%. It shows that The SSWM wrapping is more effective in M15 grade of concrete compared to M20 and M25 grade of concrete.

2. As per ACI 440.2R 2008 , the increase in load carrying capacity with one wrapping of SSWM is 46.07%, 20.70% and 5.35 for M15, M20 and M25 grade concrete columns respectively and with two wrapping it is 147.98%, 96.97% and 66.50%. As per CNR-DT 200/2004, the increase in load carrying capacity with one wrapping of SSWM is 45.01%, 35.51% and 29.30% for M15, M20 and M25 grade concrete columns respectively and with two wrapping it is 76.65%, 61.62% and 51.85%. It shows that The SSWM wrapping is more effective in M15 grade of concrete than M20 and M25 grade of concrete.

3. The ratio of axial load capacity obtained by numerical analysis and experimental work lies between 0.70 and 1.38. Similarly the ratio between axial load capacity obtained by numerical analysis and analytical work lies between 0.82 & 1.05 for ACI 440.2R and between 0.85 & 1.15 for CNR DT/200 design guidelines.

4. The increase in axial capacity for RCC circular columns is 13.96% to 24.47% with single wrapping and 47.23% to 70.87% with double wrapping for concrete of M15, M20 and M25 grade respectively. The axial load capacity of RCC columns increases by 189.61%, 203.59% and 238.32% for M15, M20 and M25 grade concrete columns from single wrapping to double wrapping.

7. Conclusions

Nonlinear FE analysis of PCC columns of 200 mm diameter, with and without SSWM wrapping, is carried out using ABAQUS software. Concrete damage plasticity model for concrete is used for FE analysis. The characteristics of stainless steel wire mesh are found experimentally and used for FE analysis. Concrete is modelled as C3D4: 4-node linear tetrahedron type of element. SSWM wrapping is modelled as S4R: 4-node doubly curved thin or thick shell, reduced integration, hourglass control, finite membrane strains element. Three sizes of finite element meshes 50 mm, 25 mm and 12.5 mm are considered for analysis. Perfect bond is assumed between concrete and SSWM. The results of analysis in terms of load-displacement curve are obtained. Comparison of load-displacement curve of PCC columns with single and double wrappings of SSWM wrapped columns is made. For analytical studies, two different guidelines namely ACI 440.2R 2008 and CNR-DT 200/2004 are used. Increase in axial load carrying capacity with increase in number of wraps, grade of concrete and different height of columns found using numerical analysis are compared with experimental results and different design guidelines. Following conclusions are drawn from numerical study:

1. As per numerical analysis, an increase in axial capacity of 15.69% to 153.95% and 13.96% to 70.87% is observed for PCC and RCC columns respectively with different number of SSWM wraps.

2. Both numerical analysis and analytical calculations using ACI 440.2R 2008, CNR-DT 200/2004 shows that the SSWM wrapping is more effective in M15 grade of concrete as compared to M20 and M25 grade of concrete. As the grade of concrete is increased, effect of SSWM wrapping is reduced.

3. The percentage increase in axial load capacity from the numerical analysis are found in agreement with ACI 440 .2R results. The CNR DT /200 results are closer to experimental results.

4. In numerical analysis, it has been observed that for various finite element mesh sizes of 12.5 mm, 25 mm and 50 mm, there is not much variation in load-displacement curves for all concrete grades and height of columns.
5. The old RCC frame structure buildings constructed with low strength concrete like M15 can be successfully strengthened with SSWM wrappings to make structures better earthquake resistant.
6. The SSWM used in numerical investigation is locally available which is much economical than CFRP/GFRP materials so can be used for axial strengthening of concrete columns with two or more wrappings at much lower costs.

References

- ABAQUS User's Manual, Ver. 6.10, Hibbit, Karlsson and Sorensen, Inc., Paw-tucket, Rhode Island.
- ACI 440.2R (2008), Guide for the Design and Construction of Externally Bonded FRP Systems for strengthening Concrete Structures, American Concrete Institute, Country Club Drive, Farmington Hills, MI 48331, U.S.A.
- Allam, S., Shoukry, M., Rashad, G. and Hassan, A. (2013), "Evaluation of tension stiffening effect on the crack width calculation of flexural RC members", *Alexan. Eng. J.*, **52**, 163-173.
- CNR-DT 200 (2004), Guide for the design and construction of Externally Bonded FRP systems for strengthening existing structures, CNR-Advisory Committee on Technical Recommendations for Construction.
- Coronado, C.A. and Lopez, M. (2007), "Damage approach for the prediction of Debonding failure on concrete elements strengthened with FRP", *J. Compos. Construct.*, **11**, 391-400.
- Gambarelli, S., Nistico, N. and Ozbolt, J. (2014), "Numerical analysis of compressed concrete columns confined with CFRP: Microplane-based approach", *Compos. Part B*, **67**, 303-312.
- Hu, B. (2013), "An improved criterion for sufficiently/insufficiently FRP-confined concrete derived from ultimate axial stress", *Eng. Struct.*, **46**, 431-446.
- Hu, D. and Barbato, M. (2014), "Simple and efficient finite element modelling of reinforced concrete columns confined with fiber-reinforced polymers", *Eng. Struct.*, **72**, 113-122.
- Hu, H.T., Lin, F.M., Liu H.T, Huang Y.F and Pan T.C. (2010), "Constitutive modelling of reinforced concrete and prestressed concrete structures strengthened by fiber-reinforced plastics", *J. Compos. Struct.*, **92**, 1640-1650.
- IRC:112 (2011), Code of practice for concrete road bridges, Indian Road Congress, New Delhi, India.
- IS 456 (2000), Plain and Reinforced concrete code of practice, Bureau of Indian Standards, New Delhi, India.
- Karabinis, A.I., Rousakis, T.C. and Manolitsi, G.E. (2008), "3D Finite-element analysis of substandard RC columns strengthened by fiber-reinforced polymer sheets", *J. Compos. Construct.*, **12**, 531-540.
- Kumar, V. and Patel, P.V. (2016), "Strengthening of axially loaded circular concrete columns using stainless steel wire mesh (SSWM)-Experimental Investigations", *Constr. Build. Mater.*, **124**, 186-198.
- Massicotte, B., Elwi, A. and MacGregor, J. (1990), "Tension-stiffening model for planar reinforced concrete members", *J. Struct. Eng.*, ASCE, **116**, 3039-3058.
- Obaidat, Y., Heyden, S. and Dahlblom, O. (2010), "The effect of CFRP and CFRP/concrete interface models when modelling retrofitted RC beams with FEM", *J. Compos. Struct.*, **92**, 1391-1398.
- Ozbakkaloglu, T., Lim, J. and Vincent, T. (2013), "FRP-confined concrete in circular sections: Review and assessment of stress- strain models", *Eng. Struct.*, **49**, 1068-1088.
- Rocca, S., Galati, N. and Nanni, A. (2008), "Review of design guidelines for FRP confinement of reinforced concrete columns of noncircular cross sections", *J. Compos. Construct.*, **12**(1), 80-92.
- Saenz, L.P. (1964), "Equation for the stress-strain curve of concrete", *ACI Struct. J.*, **61**, 1229-1235.

- Tao, Y. and Chen, J. (2014), "Concrete damage plasticity model for modelling FRP-to-concrete bond behaviour", *J. Compos. Construct.*, ASCE, **19**(1), 04014026.
- Turon, A., Davila, C., Camanho, P. and Costa, J. (2007), "An engineering solution for mesh size effects in the simulation of delamination using cohesive zone models", *Eng. Fract. Mech.*, **74**, 1665-1682.
- Zare, A. and Janghorban, M. (2013), "Shock factor investigation in a 3-D finite element model under shock loading", *Latin Am. J. Solid. Struct.*, **10**, 941-952,

CC